

This is a repository copy of *The super-chirality of vector twisted light*.

White Rose Research Online URL for this paper:

<https://eprints.whiterose.ac.uk/id/eprint/207612/>

Version: Published Version

Article:

Babiker, M. orcid.org/0000-0003-0659-5247, Yuan, J. orcid.org/0000-0001-5833-4570, Koksai, K. et al. (1 more author) (2024) The super-chirality of vector twisted light. Optics Communications. 130185. ISSN: 0030-4018

<https://doi.org/10.1016/j.optcom.2023.130185>

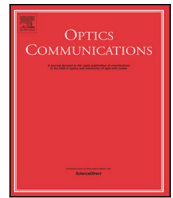
Reuse

This article is distributed under the terms of the Creative Commons Attribution (CC BY) licence. This licence allows you to distribute, remix, tweak, and build upon the work, even commercially, as long as you credit the authors for the original work. More information and the full terms of the licence here:

<https://creativecommons.org/licenses/>

Takedown

If you consider content in White Rose Research Online to be in breach of UK law, please notify us by emailing eprints@whiterose.ac.uk including the URL of the record and the reason for the withdrawal request.



The super-chirality of vector twisted light

M. Babiker^a, J. Yuan^{a,*}, K. Koksai^b, V.E. Lembessis^c

^a School of Physics, Engineering and Technology, University of York, YO10 5DD, UK

^b Physics Department, Bitlis Eren University, Bitlis, Turkey

^c Quantum Technology Group, Department of Physics and Astronomy, College of Science, King Saud University, Riyadh 11451, Saudi Arabia

ARTICLE INFO

Keywords:

Vector vortex light
Superchirality
Longitudinal component
Light-matter interaction
Enantioselectivity
Chiral selection

ABSTRACT

Vector vortex light of topological order m arises as a superposition of two twisted modes with phase functions $e^{\pm im\phi}$ (with ϕ the azimuthal variable) and circular polarizations ($\sigma = \mp 1$). We demonstrate that when m is sufficiently large these modes exhibit enhanced helicity densities when compared with the equivalent circularly-polarized Gaussian modes. The enhancement stems from the presence of longitudinal field components which become significant even for moderate beam widths. The super-chirality of light-matter interactions enabled by such modes suggests a high degree of enantioselectivity, surpassing conventional techniques for the chiral selection, so promising useful applications.

There is continued considerable interest in the physics and applications of vortex modes which are modes of light carrying orbital angular momentum despite the fact that more than three decades have now elapsed since the seminal work by Allen et al. [1] concerning light carrying orbital angular momentum. The subject now spans a number of inter-disciplinary areas, including physics, chemistry and life sciences as well as other areas, but there is still room for developments in the generation and characterization of this type of light, as in the work by Kumar et al. [2] who reported a non-interferometric method to generate various polarization singularity lattice fields. Light carrying orbital angular momentum has also featured in molecular, atomic and sub-atomic physics research and there is currently strong interest in the utility of this type of light in exploring means of detecting the chirality of matter, as demonstrated by Toyoda et al. [3] in the case of fabricated metallic nano-needles and there are suggestions that orbital angular momentum of light can affect chiral magnetic order as in metallic chiral helimagnets [4].

Recent research has highlighted the fundamental significance and the potential for applications of higher-order optical vector modes, also called higher order Poincaré (HOP) modes [5–14]. The overall polarization state of such modes is formally identified as characteristically non-separable superpositions of solutions involving circular polarization $(\hat{x} \pm i\hat{y})/\sqrt{2}$ (or $(\hat{\rho} \pm i\hat{\phi})e^{\pm i\phi}/\sqrt{2}$) and spatial phase functions $e^{\pm im\phi}$ with integer m the higher order and ϕ the azimuthal angular variable.

The case for $m = 0$ describes ordinary light with spatially uniform polarization whose vector state can be represented by a point on the well-known ordinary Poincaré sphere and covers the cases of

elliptically-polarized light (including circularly- and linearly-polarized vortex modes). The non-trivial 1st-order optical vortex modes for which $m = 1$, include radially and azimuthally polarized vector vortex modes.

Although the higher order ($m \geq 1$) vector modes have already been realized experimentally [9–11,15,16], their properties have not been explored for arbitrary order m . In particular, the question arises as to whether and how the higher order modes can offer enhanced beam properties such as higher order encoding schemes for enhanced bandwidth optical communications [17]. Similarly, it would be interesting to know whether they could lead to enhanced optical angular momentum, spin and chirality which could influence optical interaction with chiral matter [18], as optical helicity maybe enhanced through a linear combination of light beams [19]. Increased optical chirality is highly desirable for chiroptical processes [3,20]. For example, could it be the case that higher order modes would provide sufficiently strong chirality to engage effectively with chiral molecules and be able to achieve a high degree of enantioselectivity? For recent accounts on the optical interaction with chiral matter the reader is referred to [21,22].

In this communication we focus on the prospect of the existence of super-chirality, which, we envisage, maybe one of the major properties of the higher order modes. To this end, we have aimed to evaluate the helicity density and its spatial integral for the most general paraxial mode of arbitrary order m , which covers all the possible scenarios. The helicity is proportional to the optical chirality in free space and is an important pre-factor in the interaction with chiral matter [21].

* Corresponding author.

E-mail address: Jun.yuan@york.ac.uk (J. Yuan).

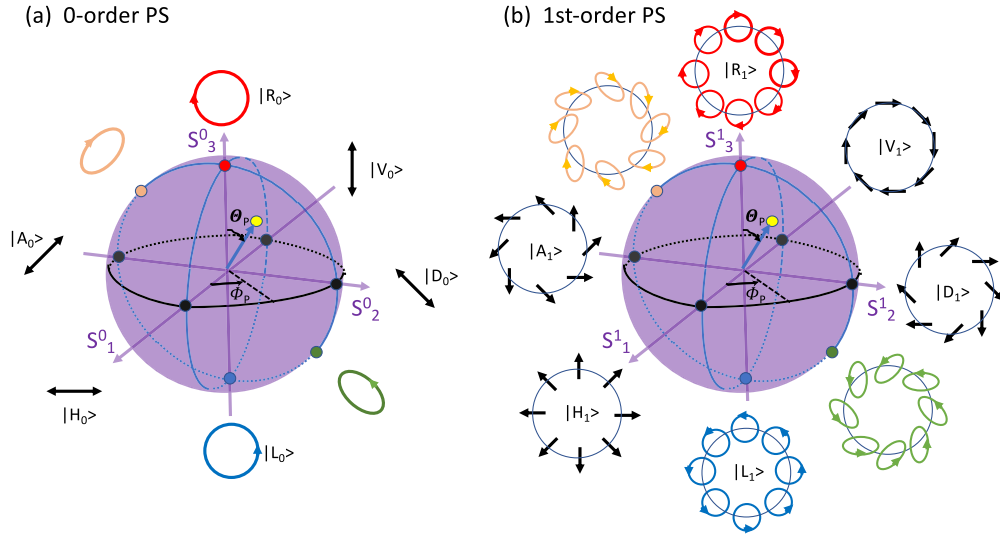


Fig. 1. 0th order, (a), and 1st-order, (b), Poincaré Sphere (PS) representation of the polarization state in which optical polarization is coupled with vortex phase (for $m \neq 0$), characterized by a unit sphere with respect to the corresponding Stokes-parameter-like Cartesian coordinates (S_1^0, S_2^0, S_3^0) and (S_1^1, S_2^1, S_3^1) respectively. It is seen that the 0th order PS is equivalent to the conventional PS where $|H_0\rangle$ and $|V_0\rangle$ are commonly used to denote the vertically and horizontally linearly polarized light, $|A_0\rangle$ and $|D_0\rangle$ for $\pm 45^\circ$ tilted linearly polarized light, $|R_0\rangle$ and $|L_0\rangle$ for right-hand and left-hand circularly-polarized light, respectively. The 1st order PS figure is related to the corresponding figure by Milione et al. [5,6] with slightly different conventions for S_1^1 and S_2^1 . Six sets of special vector modes are drawn in different colours next to each sphere for illustration. Their positions on the Poincaré sphere are indicated by filled dots of the same colour.

We start from the electromagnetic vector potential for the monochromatic vector vortex modes:

$$\mathbf{A} = \hat{\mathbf{e}}_m \tilde{F}_{m,p}(\rho) e^{ik_z z - i\omega t}, \quad (1)$$

where k_z is the axial wavevector with the light travelling along the $+z$ axis and ω is the angular frequency of the light. Also $\tilde{F}_{m,p}(\rho)$ is the amplitude function with m a positive integer and we have ignored small terms due to the Gouy and curvature phases. The ϕ -dependence is already included in the space-dependent polarization vector $\hat{\mathbf{e}}_m$ as follows [6]:

$$\hat{\mathbf{e}}_m = e^{-im\phi}(\hat{\mathbf{x}} + i\hat{\mathbf{y}})\mathcal{U}_p + e^{im\phi}(\hat{\mathbf{x}} - i\hat{\mathbf{y}})\mathcal{V}_p, \quad (2)$$

with

$$\mathcal{U}_p = \frac{1}{\sqrt{2}} \sin\left(\frac{\Theta_p}{2}\right) e^{-i\Phi_p/2}, \quad (3)$$

and

$$\mathcal{V}_p = \frac{1}{\sqrt{2}} \cos\left(\frac{\Theta_p}{2}\right) e^{i\Phi_p/2}. \quad (4)$$

Here, $\hat{\mathbf{e}}_m$ is mapped to a point (characterized by Poincaré angles Θ_p and Φ_p) on the order m Poincaré sphere. This is schematically represented in Fig. 1 for the zero order $m = 0$ and the first order $m = 1$. The Poincaré angle Θ_p spans the range from 0 to π , so that we have right-hand circular polarization at the north pole ($\Theta_p = 0$) and left-hand circular polarization at the south pole ($\Theta_p = \pi$). In-between the two pole points, we have elliptical polarizations whose degree of ellipticity changes continuously with Θ_p -values. At $\Theta_p = \pi/2$ we have linear polarization such as radial and azimuthal polarizations for $m = 1$.

The meaning of the vector vortex modes so defined becomes clear when we substitute Eq. (2) into Eq. (1). We then have

$$\begin{aligned} \mathbf{A} &= \mathcal{U}_p \mathbf{A}_1 + \mathcal{V}_p \mathbf{A}_2, \\ \mathbf{A}_1 &= (\hat{\mathbf{x}} + i\hat{\mathbf{y}}) e^{-im\phi} \tilde{F}_{m,p}(\rho) e^{ik_z z - i\omega t}, \\ \mathbf{A}_2 &= (\hat{\mathbf{x}} - i\hat{\mathbf{y}}) e^{im\phi} \tilde{F}_{m,p}(\rho) e^{ik_z z - i\omega t}. \end{aligned} \quad (5)$$

We recognize the phase functions as characteristic of optical vortex modes $e^{\mp im\phi}$, as in the case of Laguerre-Gaussian (LG) optical vortex modes [23]. So \mathbf{A}_1 and \mathbf{A}_2 describe two vortex modes: one of topological charge $-m$ with a uniform left circular polarization ($\sigma = 1$ for

$(\hat{\mathbf{x}} + i\hat{\mathbf{y}})/\sqrt{2}$) and another vortex beam of topological charge m but with a uniform right circular polarization ($\sigma = -1$ for $(\hat{\mathbf{x}} - i\hat{\mathbf{y}})/\sqrt{2}$), respectively.

The electric and magnetic fields of the generally-polarized mode are similarly written as the sums $\mathbf{B} = \mathcal{U}_p \mathbf{B}_1 + \mathcal{V}_p \mathbf{B}_2$ and $\mathbf{E} = \mathcal{U}_p \mathbf{E}_1 + \mathcal{V}_p \mathbf{E}_2$ where $\mathbf{B}_j = \nabla \times \mathbf{A}_j$; $j = 1, 2$. The sequence of next steps involves deriving first the two parts of the magnetic field and from those use Maxwell's curl B equation to derive the corresponding electric field [24]. It is easy to see that the procedure we have followed amounts to ensuring that the fields satisfy the wave equation $\nabla \times \nabla \times \mathbf{E} - \omega^2 \mathbf{E}/c^2 = 0$. This leads to corrections of the zero-order up to the first order in the paraxial approximation [25].

The \mathbf{E} and \mathbf{B} fields are needed for the evaluation of helicity which is the conserved property due to the duality symmetry of the electromagnetic field satisfying the Maxwell equation [26]. Displaying manifest duality symmetry is an important requirement of the free-space paraxial or nearly paraxial optical fields. We have found that this can be satisfied if we limit the correction to the paraxial solution to the leading order, i.e. by only including the longitudinal components of the field [25]. The dual-symmetry solutions for \mathbf{B}_1 and \mathbf{E}_1 are given by:

$$\begin{aligned} \mathbf{B}_1 &= \{k_z(\hat{\mathbf{x}} + i\hat{\mathbf{y}}) + i\hat{\mathbf{z}}(\partial_x + i\partial_y)\} e^{-im\phi} \tilde{F}(\rho) e^{ik_z z - i\omega t}, \\ \mathbf{E}_1 &= c \{ik_z(\hat{\mathbf{x}} + i\hat{\mathbf{y}}) - i\hat{\mathbf{z}}(\partial_x + i\partial_y)\} e^{-im\phi} \tilde{F}(\rho) e^{ik_z z - i\omega t}, \end{aligned} \quad (6)$$

where we have dropped the subscript label m, p in \tilde{F} for convenience and the exact notation can be restored when the need arises. For similar reasons we also drop the exponential time factor $e^{-i\omega t}$ below.

To better explore the symmetry of the vortex beams, we can express the formalism in cylindrical coordinates $\mathbf{r} = (\rho, \phi, z)$:

$$\mathbf{A}_1 = (\hat{\rho} + i\hat{\phi}) e^{-i(m-1)\phi} \tilde{F}_{m,p}(\rho) e^{ik_z z}, \quad (7)$$

$$\mathbf{A}_2 = (\hat{\rho} - i\hat{\phi}) e^{i(m-1)\phi} \tilde{F}_{m,p}(\rho) e^{ik_z z}. \quad (8)$$

Now, it is easy to see that the overall vector potential reduces to the radially- and azimuthally-polarized vector modes respectively, in the special case where $\mathcal{U}_p = \pm \mathcal{V}_p$ and $m = 1$. This can be shown explicitly when \mathbf{A}_1 and \mathbf{A}_2 describe the corresponding LG modes. Note, however, that our treatment is not restricted to the LG modes and is applicable in general to other vortex modes.

The important characteristics of the amplitudes of the longitudinal components of the field included here are their dependence on the

gradient of the transverse components of the light field. For vortex beams, this dependence can be either a radial or an azimuthal gradient, since we can write:

$$a\partial_x + b\partial_y = (a\cos\phi + b\sin\phi)\partial_\rho + \frac{b\cos\phi - a\sin\phi}{\rho}\partial_\phi, \quad (9)$$

where a and b are arbitrary constants. The key to understanding our results below is that the magnitude of the azimuthal gradient of a vortex mode is proportional to the absolute value of its topological charge $|m|$. So the contribution to the longitudinal components can come not just from radial gradients such as due to the focusing of conventional optical modes, but also due to a higher azimuthal topological charge or a higher radial order ($p > 0$) of the structured light. In the latter case, the small beam width is not an essential requirement. These aspects should now become clear by looking at the corresponding forms for \mathbf{B}_1 and \mathbf{E}_1 in purely cylindrical-coordinates. We have:

$$\mathbf{B}_1 = \left\{ k_z(\hat{\rho} + i\hat{\phi}) - i\hat{z}\left(\partial_\rho - \frac{m}{\rho}\right) \right\} e^{-i(m-1)\phi} \tilde{F}(\rho) e^{ik_z z}, \quad (10)$$

$$\mathbf{E}_1 = c \left\{ ik_z(\hat{\rho} + i\hat{\phi}) - \hat{z}\left(\partial_\rho + \frac{m}{\rho}\right) \right\} e^{-i(m-1)\phi} \tilde{F}(\rho) e^{ik_z z}, \quad (11)$$

where c is the speed of light. We see that the z -component of both the magnetic and electric fields have the $e^{-i(m-1)\phi}$ phase factor, consistent with the spin-orbit conversion first found for Bessel beams [27].

Similarly, the fields \mathbf{B}_2 and \mathbf{E}_2 emerge following exactly the same procedure as followed for \mathbf{B}_1 and \mathbf{E}_1 . We obtain:

$$\mathbf{B}_2 = \left[k_z(\hat{\rho} - i\hat{\phi}) + i\hat{z}\left(\partial_\rho - \frac{m}{\rho}\right) \right] e^{i(m-1)\phi} \tilde{F}(\rho) e^{ik_z z}, \quad (12)$$

$$\mathbf{E}_2 = c \left[ik_z(\hat{\rho} - i\hat{\phi}) - \hat{z}\left(\partial_\rho + \frac{m}{\rho}\right) \right] e^{i(m-1)\phi} \tilde{F}(\rho) e^{ik_z z}. \quad (13)$$

Having obtained expressions for the fields, we are now ready to evaluate the cycle-averaged optical densities of the helicity $\bar{\eta}$ and chirality $\bar{\chi}$ which are defined by

$$\bar{\eta}(\mathbf{r}) = -\frac{\epsilon_0 c}{4\omega} \Im[\mathbf{E}^* \cdot \mathbf{B}] = \frac{c}{\omega^2} \bar{\chi}, \quad (14)$$

where ϵ_0 is the permittivity constant in free space. $\mathbf{E}^* \cdot \mathbf{B}$ can be expanded into four terms involving \mathbf{E}_j and \mathbf{B}_j , with $j = 1, 2$ as given above. The symbol $\Im[\dots]$ in Eq. (14) stands for the imaginary part of $[\dots]$ and the superscript $*$ in \mathbf{E}^* stands for the complex conjugate of \mathbf{E} . In what follows, we focus on the helicity density from which the corresponding optical chirality density $\bar{\chi}$ can be determined using Eq. (14). We find after some algebra

$$\bar{\eta}(\mathbf{r}) = \frac{\epsilon_0 c^2}{4\omega} \cos(\Theta_p) \left\{ 2k_z^2 |\tilde{F}_{m,p}|^2 + |\tilde{F}'_{m,p}|^2 + m^2 \frac{|\tilde{F}_{m,p}|^2}{\rho^2} + 2m \frac{\tilde{F}'_{m,p} \tilde{F}_{m,p}}{\rho} \right\}, \quad (15)$$

where we have set $\tilde{F}' = d\tilde{F}/d\rho$. This is the most general result for the helicity density of a vector vortex mode of any order m . Note that it shows no dependence on Φ_p , i.e. all points on a given latitude for which $0 \leq \Phi_p \leq 2\pi$ have the same helicity density.

It turns out that the interference terms $\mathbf{E}_1^* \cdot \mathbf{B}_2$ and $\mathbf{E}_2^* \cdot \mathbf{B}_1$ did not contribute to the helicity density of the vector vortex beams displayed in Eq. (15) and only the two direct terms $\mathbf{E}_1^* \cdot \mathbf{B}_1$ and $\mathbf{E}_2^* \cdot \mathbf{B}_2$ contribute. This is understandable as the constituent 1 and 2 are orthogonal eigenmodes.

We can re-express the helicity density displayed in Eq. (15) for an arbitrary optical vector vortex mode in terms of the helicity density $\bar{\eta}_1$ or $\bar{\eta}_2$ associated with the two special points on the higher order Poincaré sphere, namely the vortex modes of the same order but with a uniform circular polarization, corresponding to $\Theta_p = 0, \pi$. The helicity density for this type of vortex mode with uniform circular polarization has already been studied in [28].

The physical meaning of the four terms within the curly brackets in the helicity density expression shown in Eq. (15) can now be understood with reference to the expression for the corresponding \mathbf{E} and \mathbf{B} -fields.

The first term in Eq. (15) can be identified with the helicity density for a zero-order mode with a general elliptical polarization, corresponding to $m = 0$. The second term is associated with the part of the longitudinal component of the mode and we note that it depends on the field radial gradient. The rest of the terms are the m -dependent and are characteristic of vector vortex modes. The term proportional to \tilde{F}^2 can be seen to arise from the azimuthal phase gradient, while the term proportional to $\tilde{F}'\tilde{F}$ is the hybrid term involving contributions from cross terms involving the radial and azimuthal gradients, hence the m -dependence.

The cycle-averaged helicity density $\bar{\eta}$ is a key parameter determining the strength of the interaction of the light mode with a chiral object, for example the optical dichroic response in a homogeneous chiral medium arises via $\kappa\bar{\eta}$ where κ is the optical chirality parameter of a linear response matter [21]. Superhelicity is normally defined as the excess helicity with respect to circularly-polarized plane waves, which can be approximated in our case by that of a non-vortex ($m = 0$) mode of very large beam width. This shows trivially that the helicity, hence chirality, is enhanced at the position of the peak intensity of a mode with a narrower beam width. To show superhelicity, hence the possibility of superchiral interaction, we look for the excess contribution arising from the last three terms in Eq. (15). The first term is well known and can be induced by tight focusing of the beam [28]. The more interesting terms are the last two m -dependent terms as the topological charge of the vortex mode can be made very large, with the potential for a superchiral interaction compared with the case of a non-vortex mode. This can be achieved even for moderately focused beams because its contribution to the longitudinal terms is independent of the contribution from tight focusing.

We may now demonstrate the super-chirality properties of higher order modes for the special case of Laguerre-Gaussian modes of waist w_0 , which has an amplitude function given as follows

$$\tilde{F}_{m,p}(\rho) = \mathcal{A}_0 \sqrt{\frac{p!}{(p+|m|)!}} e^{-\frac{\rho^2}{w_0^2}} \left(\frac{\sqrt{2}\rho}{w_0} \right)^{|m|} L_p^{|m|} \left(\frac{2\rho^2}{w_0^2} \right) \quad (16)$$

where L_p^m is the associated Laguerre polynomial of indices m and p . The overall factor \mathcal{A}_0 is a normalization constant which is determined in terms of the applied power P_T , evaluated as the integral of the z -component of the Poynting vector over the beam cross-section. We have

$$P_T = \frac{1}{2\mu_0} \int_0^{2\pi} d\phi \int_0^\infty |(\mathbf{E}^* \times \mathbf{B})_z| \rho d\rho = \left(\frac{\pi\omega^2\epsilon_0 c w_0^2}{4} \right) \mathcal{A}_0^2 \quad (17)$$

Fig. 2 displays the helicity density for the cases $m = 0, 1, 12, 36$ and 150 for $\Theta_p = 0$. It is clear that for $m = 0$ and $m = 1$ the helicity density is maximum on axis ($\rho = 0$) and that the case $m = 1$ is larger than that for $m = 0$, which makes the case $m = 1$ super-chiral. For $m > 1$ the density is concentrated off-axis ($\rho > 0$). The peak value initially decreases with increasing m , but it then increases and becomes larger than the case $m = 0$ again.

The super-chirality feature at the core $\rho = 0$ for $m = 1$ can be explained as follows. This density is proportional to dot product of \mathbf{E}^* and \mathbf{B} . It is thus the sum of two dot products: (1) the product of the transverse components $\mathbf{E}_T^* \cdot \mathbf{B}_T$ and (2) the product of longitudinal parts $E_z^* B_z$. The product of the transverse components has a vortex structure, hence it is zero at the core, but the longitudinal parts have a non-zero-value at the core. That this occurs for $m = 1$ is consistent with the requirement that $m + \sigma = 0$ and is due to the inclusion of the longitudinal field components.

This can also be explained analytically by inspecting the terms which appear in Eq. (15). When applied to the Laguerre-Gaussian $\tilde{F}(\rho)$

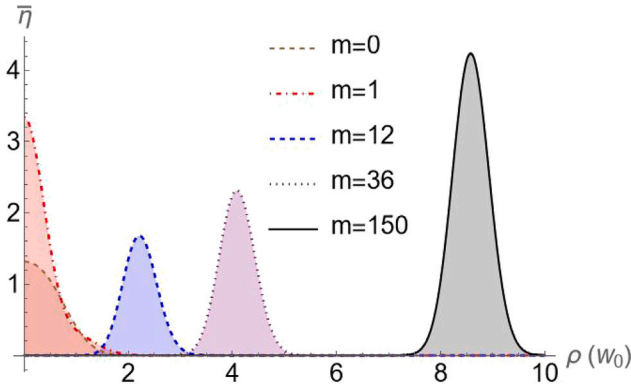


Fig. 2. Variations with ρ/w_0 of the helicity density, $\bar{\eta}$, Eq. (15) (arbitrary units), due to modes of orders $m = 0, 1, 12, 36$ and 150 . The plots concern circularly-polarized Laguerre-Gaussians for which $\cos(\Theta_p) = +1$. A mode is said to be super-chiral when its helicity density at maximum value exceeds that for $m = 0$ (shaded brown, maximum on axis). Clearly the large value in the case $m = 150$ (shaded black) is highly super-chiral.

for $m = 1$, we have from Eq. (16) $|\tilde{F}_{m=1}|^2 \propto \rho^2$ and also we have $[\tilde{F}'\tilde{F}]_{m=1} \propto \rho$. Once substituted in the relevant terms in the helicity density we see that the factor $1/\rho^2$ in the first term cancels the factor ρ^2 in the numerator and the $1/\rho$ in the second term cancels with the factor ρ in the numerator. The overall variation amounts to a non-zero value of the helicity at $\rho = 0$ for $m = 1$. This variation contrasts with the case $m \geq 2$ in which the numerators in the two terms have higher powers of ρ , guaranteeing that the helicity density vanishes at $\rho = 0$.

We can evaluate the total integral of the helicity density in Eq. (15) over the transverse plane. First we note that the radial integral of all terms in the form $\frac{\tilde{F}'\tilde{F}}{\rho}$ are identically zero for all mode functions which satisfy $\tilde{F}_{m,p}(0) = 0 = \tilde{F}_{m,p}(\infty)$. The contribution of the term proportional to m^2 requires the evaluation of the following integral

$$I_m = \int_0^\infty \rho d\rho \left[\frac{1}{\rho^2} |\tilde{F}_{m,p}|^2 \right] = \frac{1}{2m} \quad (18)$$

We find, after some algebra, that the total helicity per unit length of order m vector vortex mode is given by

$$\bar{C}_m = \mathcal{L}_0 \cos(\Theta_p) \left(1 + \frac{(m+1)\bar{\lambda}^2}{w_0^2} \right) \quad (19)$$

where $\bar{\lambda} = \lambda/(2\pi)$, $\mathcal{L}_0 = P_T/(k_z c^2)$ is a constant for a fixed power P_T and we have substituted for \mathcal{A}_0 using Eq. (17). It is easy to check that the \bar{C}_m has the dimensions of angular momentum per unit length. Note that although the factor $\bar{\lambda}^2/w_0^2$ in Eq. (19) is typically small for $w_0 \gg \bar{\lambda}$, the higher order helicity for which $m \gg 1$ would ensure super-chirality for relatively large w_0 .

The constitutive relations for a homogeneous chiral medium characterized by a linear optical response are as follows [21]:

$$\mathbf{D} = \epsilon_r \epsilon_0 \mathbf{E} + \frac{i\kappa}{c} \mathbf{H}, \quad (20)$$

$$\mathbf{B} = -\frac{i\kappa}{c} \mathbf{E} + \mu_r \mu_0 \mathbf{H}, \quad (21)$$

where ϵ_r is the relative permittivity, μ_r the relative permeability, \mathbf{D} the electrical displacement, \mathbf{H} the magnetic field intensity and, crucially, κ the optical chirality parameter of the medium which is related to the magnetoelectric dipolar polarizability. Tang and Cohen [18] demonstrated (for circularly-polarized lights, corresponding to $m = 0$, $\Theta_p = 0$ and π), that the helicity (and chirality) density of light is a useful local measure of the asymmetry in the optical excitation of a chiral molecule and its chiral counterpart. For example, absorption in the dipole approximation is given by $a_E |\mathbf{E}|^2 + a_H |\mathbf{H}|^2 + b\bar{\eta}$, where a_E , a_H and b are proportionality constants and $\bar{\eta} \propto \cos\Theta_p = \pm 1$ for circularly-polarized light of opposite handedness. Using a similar

argument, Canaguier-Durand et al. [29] and Cameron et al. [19] have shown that the corresponding optical force exerted upon a small chiral molecule has the form $\vec{F} = a'\nabla w + b'\nabla\bar{\eta}$, where w is the local energy density associated with the achiral dipole force and a' and b' are proportionality constants. In both cases, the chirality density of light described here only applies to chiral materials with electrical dipole and magnetic dipole interactions [18,19]. This means that it only applies to chiral objects whose size is much smaller than the wavelength of the light and is such that multipolar effects are not important. Our treatment also applies to chiral metamaterials (see Ref. [30] for example) as long as the constituent feature size is much smaller than the wavelength of the light used. Our treatment is also limited to weak fields such that non-linear interactions can be ignored.

As the same physical description that applies to the chiroptical response of matter that is illuminated by circularly polarized light also applies to the HOP modes described in this paper, we envisage that the experiments involving a dichroic response of homogeneous media, such as a solution containing chiral molecules, with circularly-polarized light, may be readily modified by replacing the ordinary circularly-polarized light with the light at the opposite polar regions of the HOP spheres, in order to achieve an enhanced chiral response. Similarly, an enantiomer-selective dipole force can be used in the spatial separation of molecules according to their chirality. Such experiments are now realistic in view of the availability of HOP mode lasers [10] or other similar HOP mode light sources.

In conclusion, we have evaluated the helicity (and the chirality) density for general paraxial vector vortex modes in which the state of polarization is specified by a general point (Θ_p, Φ_p) on the surface of the order m Poincaré unit sphere, where m is a positive integer. The general results obtained encompass a wide range of scenarios governed by their dependence on the Poincaré sphere angles, the mode amplitude function and the higher order m . In particular, the helicity (and the chirality) density is found to be proportional to terms involving m and m^2 , which means that the higher order modes exhibit super-chirality when compared that of an ordinary (order $m = 0$) elliptically polarized mode. Specifically, we have also shown that the first order $m = 1$ mode is a markedly superchiral vortex mode which is dominated by the vortex core at $\rho = 0$. We have also found that other higher modes for which $m > 1$ have off-axis maximum helicity which is also superchiral. These results strongly indicate the existence of a highly desirable super-chirality property of the vector vortex modes which, we suggest, is now ripe for direct experimental investigation.

Declaration of competing interest

The authors declare that they have no known competing financial interests or personal relationships that could have appeared to influence the work reported in this paper.

Data availability

No data was used for the research described in the article.

References

- [1] L. Allen, M.W. Beijersbergen, R. Spreeuw, J. Woerdman, Phys. Rev. A 45 (1992) 8185.
- [2] P. Kumar, S.K. Pal, N.K. Nishchal, P. Senthilkumar, J. Opt. Soc. Amer. A 37 (2020) 1043.
- [3] K. Toyoda, F. Takahashi, S. Takizawa, Y. Tokizane, K. Miyamoto, R. Morita, T. Omatsu, Phys. Rev. Lett. 110 (2013) 143603.
- [4] Y. Goto, H. Ishihara, N. Yokoshi, New J. Phys. 23 (2021) 053004.
- [5] G. Milione, Vector Beams for Fundamental Physics and Applications (Ph.D. thesis), New York, USA, 2016.
- [6] G. Milione, H.I. Sztul, D.A. Nolan, R.R. Alfano, Phys. Rev. Lett. 107 (2011) 053601.
- [7] E.J. Galvez, B. Khajavi, B.M. Holmes, in: M.D. Al-Amri, D.L. Andrews, M. Babiker (Eds.), Structured Light for Optical Communication, in: Nanophotonics, Elsevier, 2021, pp. 95–106.

- [8] C. Maurer, A. Jesacher, S. Fürhapter, S. Bernet, M. Ritsch-Marte, *New J. Phys.* 9 (2007) 78.
- [9] Y. Liu, X. Ling, X. Yi, X. Zhou, H. Luo, S. Wen, *Appl. Phys. Lett.* 104 (2014) 191110, <http://dx.doi.org/10.1063/1.4878409>.
- [10] D. Naidoo, F.S. Roux, A. Dudley, I. Litvin, B. Piccirillo, L. Marrucci, A. Forbes, *Nat. Photonics* 10 (2016) 327.
- [11] Z. Liu, Y. Liu, Y. Ke, Y. Liu, W. Shu, H. Luo, S. Wen, *Photon. Res.* 5 (2017) 15.
- [12] Q. Zhan, *Adv. Opt. Photonics* 1 (2009) 1.
- [13] G. Volpe, D. Petrov, *Opt. Commun.* 237 (2004) 89.
- [14] B.M. Holmes, E.J. Galvez, *J. Opt.* 21 (2019) 104001.
- [15] Y. Shen, Z. Wang, X. Fu, D. Naidoo, A. Forbes, *Phys. Rev. A* 102 (2020) 31501.
- [16] C. Chen, Y. Zhang, L. Ma, Y. Zhang, Z. Li, R. Zhang, X. Zeng, Z. Zhan, C. He, X. Ren, C. Cheng, C. Liu, *Opt. Express* 28 (2020) 10618.
- [17] M.D. Al-Amri, D.L. Andrews, M. Babiker, *Structured Light for Optical Communication*, Elsevier, 2021.
- [18] Y. Tang, A.E. Cohen, *Phys. Rev. Lett.* 104 (2010) 163901.
- [19] R.P. Cameron, S.M. Barnett, A.M. Yao, *J. Modern Opt.* 16 (2014) 25.
- [20] J. Feis, D. Beutel, J. Köppler, X. Garcia-Santiago, C. Rockstuhl, M. Wegener, I. Fernandez-Corbaton, *Phys. Rev. Lett.* 124 (2020) 033201.
- [21] J. Mun, M. Kim, Y. Yang, T. Badloe, J. Ni, Y. Chen, C.-W. Qiu, J. Rho, *Light Sci. Appl.* 9 (2020) 139.
- [22] C. Genet, *ACS Photonics* 9 (2022) 319.
- [23] D.L. Andrews, M. Babiker (Eds.), *The Angular Momentum of Light*, Cambridge University Press, Cambridge, 2012.
- [24] H.A. Haus, *Waves and Fields in Optoelectronics*, Prentice Hall, 1984.
- [25] M. Lax, W.H. Louisell, W.B. McKnight, *Phys. Rev. A* 11 (1975) 1365.
- [26] R.P. Cameron, S.M. Barnett, A.M. Yao, *New J. Phys.* 14 (2012) 053050.
- [27] K.Y. Bliokh, M.A. Alonso, E.A. Ostrovskaya, A. Aiello, *Phys. Rev. A* 82 (2010) 063825.
- [28] M. Babiker, J. Yuan, V. Lembessis, K. Koksai, *Opt. Commun.* 525 (2022) 128846.
- [29] A. Canaguier-Durand, J.A. Hutchison, C. Genet, T.W. Ebbesen, *New J. Phys.* 15 (2013) 123037.
- [30] Z. Hu, N. He, Y. Sun, Y. Jin, S. He, *Prog. Electromagn. Res.* 172 (2021) 51.